



# Mixing along the Red Giant Branch

Achim Weiss<sup>1</sup> and Corinne Charbonnel<sup>2,3</sup>

<sup>1</sup> Max-Planck-Institut für Astrophysik, Karl-Schwarzschild-Str. 1, 85748 Garching, Germany e-mail: aweiss@mpa-garching.mpg.de

<sup>2</sup> Geneva Observatory, 51 Chemin des Maillettes, 1290 Sauverny, Switzerland e-mail: Corinne.Charbonnel@obs.unige.ch

<sup>3</sup> Laboratoire d'Astrophysique de l'Observatoire Midi-Pyrénées, 14 av. Belin, 31400 Toulouse, France

**Abstract.** We review canonical mixing in low-mass stars on the Red Giant Branch, the evidence for additional – extra – mixing based on observations of chemical abundance trends and anomalies, discuss the connection with the Red Giant bump and with proton-nucleosynthesis, and the current understanding of the connection between extra-mixing and differential rotation. New developments concerning the sequence of events leading to the observed abundances are included, too.

**Key words.** low-mass stars – Red Giants – chemical abundances – mixing – rotation

## 1. Canonical stellar evolution

Stars with masses below  $\approx 2 - 2.5 M_{\odot}$  evolve along the Red Giant Branch to high luminosities until helium burning is ignited in their core under degenerate conditions. Already at the beginning of the Red Giant phase the photospheric abundances of carbon and nitrogen, and the isotope ratio  $^{12}\text{C}/^{13}\text{C}$  change. These effects are consequences of the *first dredge-up* (1<sup>st</sup> du, Iben 1965), which is the only mixing event predicted by canonical stellar evolution theory for low-mass stars during the main-sequence and Red Giant phase.

The evolution starts with central hydrogen burning on the main-sequence. Due to the rather low core temperatures, proton-nucleosynthesis affects only the nuclei involved in the *pp*-chain and CNO-cycle, the lat-

ter being dominant for stellar mass above  $\approx 1.3 M_{\odot}$  only. However, even for the lower mass range of, say  $0.7 - 0.9 M_{\odot}$ , the initial C  $\rightarrow$  N conversion takes place, although the whole cycle (involving changes in O) is completed only rarely. Nuclei of higher cycles, such as those of the NeNa and MgAl cycles, are not affected. At the end of the main-sequence when central burning shifts to shell burning, the hydrogen-burning shell establishes itself within the former burning core, such that above the shell we find a region of composition modified by H-burning: a  $^{12}\text{C}/^{13}\text{C}$  value close to the equilibrium value of  $\approx 3$ , almost vanishing carbon, and strongly enhanced nitrogen abundance. In addition,  $^3\text{He}$  is increased by huge factors in those regions of the former core where temperature was low enough for a high  $^3\text{He}$ -abundance within the *pp*-chain, but high enough for nuclear reactions establishing the equilibrium quickly (Clayton 1983). Finally,

*Send offprint requests to:* Achim Weiss

*Correspondence to:* Achim Weiss

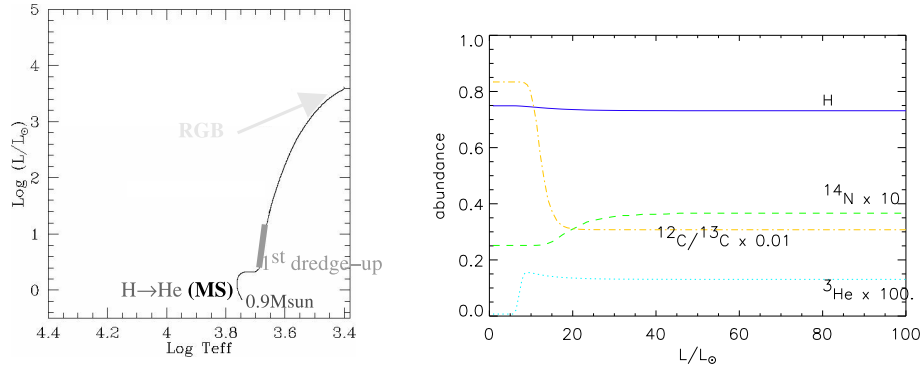


**Fig. 1.** The 1<sup>st</sup> du during the evolution of a metal-poor star of  $0.9 M_{\odot}$ ; left: HRD; right: corresponding changes of surface abundances.

${}^7\text{Li}$  is strongly depleted over a large fraction of the stellar interior, due to its low  $p$ -capture temperature of  $\approx 2.5 \cdot 10^6$  K.

As the star becomes cooler on the subgiant and early red giant branch, the envelope convection deepens until it touches these regions and mixes the modified material to the surface. This and the resulting changes in element and isotope abundances (as predicted from evolutionary models) is shown in Fig. 1. After the 1<sup>st</sup> du the convective envelope retreats ahead of the advancing hydrogen-shell and no further changes in the surface abundances is predicted.

This picture is supported by observations, the most impressive data coming from Gratton et al. (2000) for field stars with accurate *Hipparcos* parallaxes.<sup>1</sup> The strength of the 1<sup>st</sup> du increases with decreasing metallicity, with mass up to  $\approx 1 M_{\odot}$ , decreasing again for higher masses, and with decreasing initial helium content. It also leads to a slight enrichment of the convective envelope with helium. For more massive stars, the energy generation of which is dominated by the CNO-cycle, a slight decrease in oxygen would be expected, too.

<sup>1</sup> The corresponding figure has been shown several times during this meeting, such that we refer the reader to the corresponding contributions by Snenen, Denissenkov, and others.

## 2. Observational evidence for extra-mixing

Gratton et al. (2000) not only demonstrated the reality of the 1<sup>st</sup> du as predicted consistently by all stellar evolution calculations, but – more importantly – showed that in field stars a further decrease of  ${}^7\text{Li}$ , C,  ${}^{12}\text{C}/{}^{13}\text{C}$ , and an accompanying increase in N takes place along the upper RGB. This additional evolutionary effect can be fully accounted for by requiring an additional – extra – mixing between the bottom of the convective envelope and the outermost layers of the advancing hydrogen-shell. The shell is always hot enough for CNO-burning being the main energy source, and thus the CN-conversion takes place in regions outside the major energy producing layers. This explanation of the abundance changes by a postulated mixing of CN-subcycle material from the outermost shell region, had been proposed already by Sweigart & Mengel (1979).

The observations of the field stars also demonstrate that the extra-mixing has a well-defined starting point along the RGB: the so-called RGB-bump (Charbonnel et al. 1998). Physically, it is the point where the hydrogen burning shell encounters the deepest point to which the convective envelope ever reached, and where the hydrogen content shows a sudden increase. As a consequence of the increase of fuel, the star exhibits a short downward loop in the HRD, after which the upward evolution

resumes. The result is a higher probability to find a star in this brightness bin, and therefore luminosity functions of globular clusters show a bump. Theory and observation nicely agree about the size and location (around  $\log L/L_{\odot} = 2$ ) of the bump (e.g. Zoccali et al. 1999).

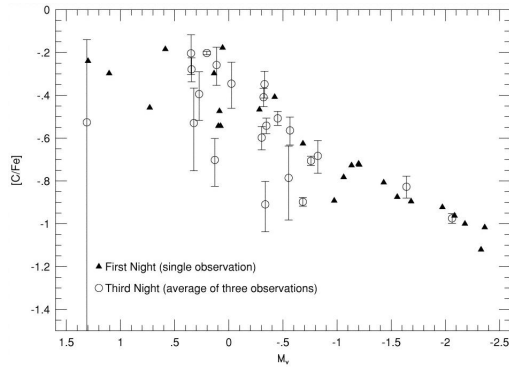


**Fig. 2.** [C/Fe] as function of brightness along the RGB of the cluster M92 (Bellman et al. 2001).

Since the late eighties similar C/N-abundance variations have also been found in Globular Clusters (see Kraft 1994 for a review on the early results). The clearest evidence that this is an evolutionary effect is found in M92 (Bellman et al. 2001, see Fig. 2). Again, it has been confirmed that the extra-mixing starts at the bump, for example in NGC 6752, where Grundahl et al. (2002) found additional Li-depletion setting in at the bump, or in terms of the  $^{12}\text{C}/^{13}\text{C}$  ratio in four clusters (Shetrone 2003).

Finally, since the work by Gilroy (1989) and Gilroy & Brown (1991 M67) it has been known that also in Open Clusters  $^{12}\text{C}/^{13}\text{C}$  falls well below the 1<sup>st</sup> du prediction such that the presence of additional mixing was claimed. Figure 3 shows that both in clusters and field stars  $^{12}\text{C}/^{13}\text{C}$  falls with brightness and that the effect is independent of metallicity for  $[\text{Fe}/\text{H}] < -1$  (from Charbonnel & do Nascimento 1998).

Therefore, we conclude this section by summarizing that the abundance variations of Li, C, N, and carbon isotopes, seen in low-mass

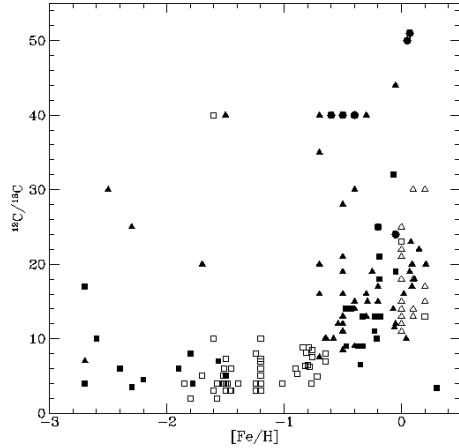


**Fig. 3.**  $^{12}\text{C}/^{13}\text{C}$  as a function of  $[\text{Fe}/\text{H}]$  for a collection of field (filled) and cluster (open symbols) giants. Circles:  $M_V > 2$ , triangles:  $0 < M_V < 2$ , quares:  $M_V < 0$  (from Charbonnel & do Nascimento 1998).

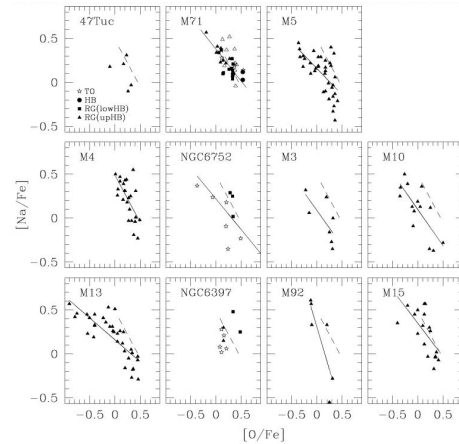


**Fig. 4.** Na–O anticorrelation in GCs (Ramírez & Cohen 2002)

red giants can be consistently explained by an extra-mixing process that sets in at the bump and that mixes material from the outer layers of the hydrogen-burning shell to the bottom of the convective envelope. This extra-mixing appears to be nearly universal, independent of the star's environment, its metallicity (although the amount of mixing increases with decreasing metallicity), and mass, as long as it is low

enough. This process has not been identified rigidly so far, but see Sect. 4 for promising models.

### 3. Further abundance anomalies

Since a decade it has been known that in addition to the elements discussed so far, also others (O, Na, Mg, Al) show variations in globular cluster red giants (see Kraft et al. 1993 for an early paper and Ramírez & Cohen 2002 for a recent compilation of known cases; see Fig. 4). In particular, an overabundance of Na in correlation with a depletion of O is found; this O–Na anticorrelation is most pronounced in M13, where the O-deficit amounts to 1 dex in some stars. Denissenkov & Denissenkova (1990) showed that the Na-overabundance could be explained by assuming that we see matter processed in the NeNa-cycle of hydrogen fusion, where Na is enriched in analogy to N in the CNO-cycle. While the depleted  $^{22}\text{Ne}$  cannot be observed, the NeNa-cycle takes place at temperatures, where O is depleted in the CNO-cycle, too (around  $\delta m \approx 0.1$  in Fig. 5). The Na–O–anticorrelation is therefore understandable in terms of  $p$ -nucleosynthesis. Contrary to the CN-case, however, no clear evolutionary trend along the RGB was found, except possibly for M13 (Weiss et al. 2000, Sneden, these proceedings). The extent of the anticorrelation seems to reflect just the burning temperature to which the matter had been exposed.

Indeed, Gratton et al. (2001, Gratton, these proceedings) convincingly detected the same range of O and Na variation in both turn-off and subgiant stars in NGC 6752, that is, long before the universal deep-mixing mechanism is believed to set in. In addition, since burning temperatures on the main-sequence are too low for the NeNa-cycle to operate, the observed variations cannot be of intrinsic nature, but must be already in the initial main-sequence composition (*primordial*). Ramírez & Cohen (2002) confirmed this fact for another cluster (M71). Therefore, while  $p$ -nucleosynthesis is still the underlying explanation for the O and Na anomalies, it appears that this is not an intrinsic effect of the stars displaying it.

There is another significant difference compared to the CN-anomaly: field stars with an ONa-anticorrelation have not been detected so far in spite of dedicated observations Gratton et al. (2000) and large literature searches (Charbonnel et al. 2003; see Fig. 6). Environment, therefore, seems to have a crucial influence of the occurrence of the O–Na-anticorrelation.

Finally, yet another anomaly is known, affecting Mg and Al (see Ivans et al. 1999 for a collection of data). At moderate Mg-deficiency, huge Al-overabundances up to 1 dex have been found. While again this can be explained in terms of  $p$ -nucleosynthesis (see Langer & Hoffman 1995), burning temperatures of 70 MK and above are needed for the variations observed. Such temperatures are encountered in AGB-stars only (see, therefore, the corresponding contributions to this meeting). Grundahl et al. (2002) and Ramírez & Cohen (2002) found the anomalies present in early evolutionary phases in NGC 6752 and M71, strengthening the case for a primordial source, either as the only reason (D’Antona, this meeting) or together with deep mixing

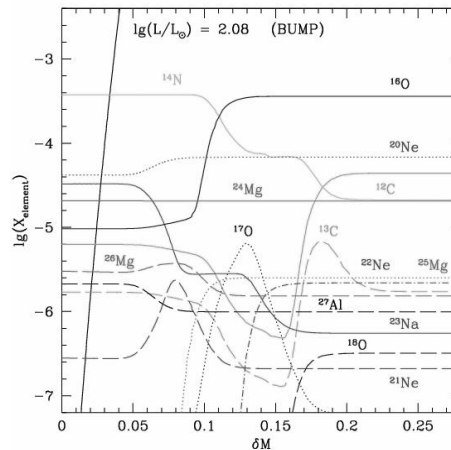


**Fig. 5.** Abundances within the hydrogen-burning shell as function of relative mass  $\delta m$ , defined as ranging from 0 to 1 between the bottom of the shell and the convective envelope.

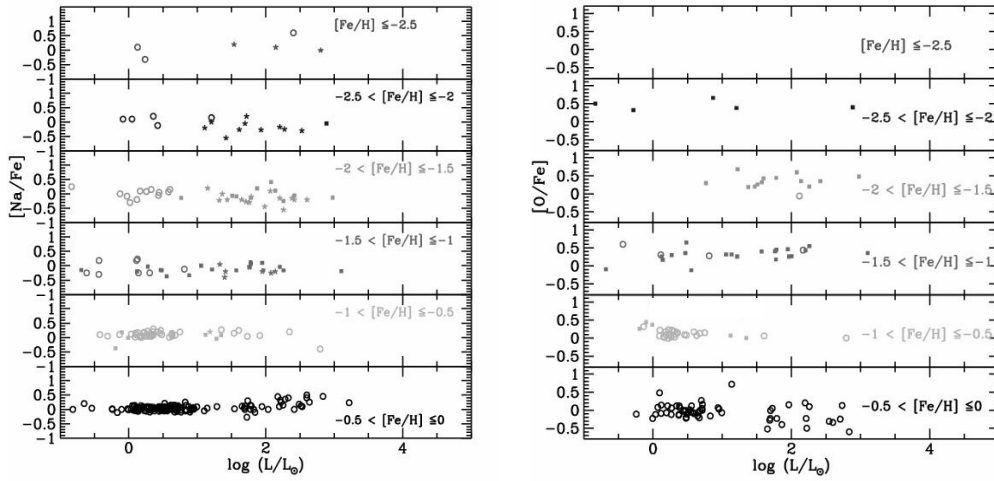


**Fig. 6.** Na and O in 625 field stars of different  $[\text{Fe}/\text{H}]$  as function of luminosity; while scatter is visible, no trend or anticorrelation is detectable (Charbonnel et al. 2003, in preparation).

events (Denissenkov et al. 1998). As in the case of Na-O, Charbonnel et al. (2003, in preparation) find no evidence for similar effects in field stars. The conclusion of all these abundance anomalies, which can be linked to proton-nucleosynthesis, is that the universal deep mixing affects only the  $pp$ - and CNO-nuclei, a fact which immediately allows to restrict the depth of penetration into the shell to  $\delta m \gtrsim 0.12$  (Fig. 5). Let us mention the recent determination of the oxygen isotopic ratios in a couple of RGB stars with low carbon isotope ratio (Balachandran & Carr 2003), which reinforces this result. In these objects, both the  $^{16}\text{O}/^{17}\text{O}$  and  $^{16}\text{O}/^{18}\text{O}$  ratios are high, in agreement with extensive CN-processing but no dredge-up of ON-cycled material in RGB stars. However, deeper mixing in individual stars or clusters (M13) is not excluded.

## 4. Modelling deep mixing

### 4.1. Parametric mixing

At the present time, we have no rigid physical model for the deep mixing with predictive power, though rotation as the basic cause

is being investigated thoroughly (see Sect. 4.2, 4.3). As early as Sweigart & Mengel (1979) matter flows as a consequence of rotation have been suggested to explain the CN-variations, initially as meridional circulation, later also including the interaction with differential rotation and shear.

For fast and easy stellar evolution calculations, however, parametrized approaches have proved to be capable of reproducing individual observations. Some examples are Wasserburg et al. (1995), Cavallo et al. (1996), Boothroyd & Sackmann (1999). The individual assumptions and technical realizations differ, but the principal idea is always very similar. In the following we will discuss the approach by Denissenkov & Weiss (1996 and later work).

Here, the mixing is treated as a diffusion process, with the diffusive velocity (or diffusion constant  $D_{\text{mix}}$ ) estimated from meridional circulation ( $D_{\text{mix}} \approx 10^8 \dots 10^{10} \text{ cm}^2/\text{s}$ ). The mixing depth is a second free parameter expressed in the relative mass coordinate  $\delta m$ . Stellar models *without deep mixing* are calculated and taken as background structures for the separate calculation of deep mixing and complete  $p$ -nucleosynthesis. It is assumed

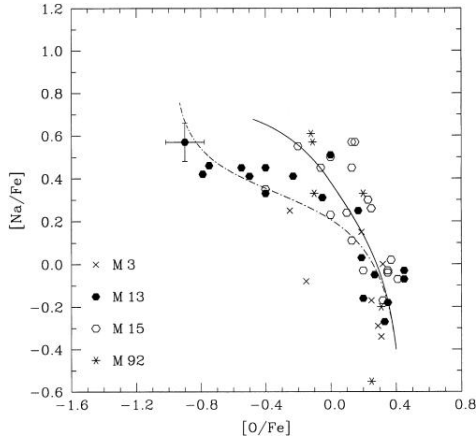


**Fig. 7.** O–Na-anticorrelation in giants of several clusters (see legend) and results of two models to reproduce it (Denissenkov & Tout 2000); dash-dotted line: parametric model with  $\delta m = 0.06$  and  $D_{\text{mix}} = 2.5 \cdot 10^9 \text{ cm}^2/\text{s}$ ; solid: rotation model (see text).

that the effect of deep mixing does not alter the background evolution significantly, as well as that the restriction to  $pp$ - and CNO-nucleosynthesis in the full models is justified. This lack of consistency is still an open matter of debate, and will be solved only with fully consistent models in the future. For the reproduction of the observed (anti-)correlations the models seem to be sufficient, though. At least for extremely deep mixing, which leads to significant He-changes in the envelope the parametric mixing has been included in full stellar models (Weiss et al. 2000). Recall that the ONa-anticorrelation needs to be explained in large parts by a primordial effect. However, the parametric deep mixing models confirmed the H-shell in red giants as the possible nucleosynthetic site of origin.

With these models, the carbon depletion, the decline of  $^{12}\text{C}/^{13}\text{C}$  and even the O–Na-anticorrelation could be reproduced in all cases, demonstrating that shell-nucleosynthesis in red giants and mixing are fully sufficient to explain the observations. In Fig. 7 (dash-dotted line) we show the result of such a calculation, even if now a primordial scenario seems to be more realistic (Sect. 3)

for this particular abundance (anti-)correlation. Two points are worth to be emphasized: 1. The line in Fig. 7 is the result of an evolutionary effect, starting in the lower right corner (no anomaly) and developing to the maximum extent of the anomaly. However, the data points, while bracketing the full extent of the abundance variations, do not correspond to any evolutionary sequence. The comparison therefore suggests a better agreement than there really might be. 2. The parameters needed to explain CN-, resp. ONa-variations are different (mainly  $\delta m$ , see Fig. 5). The observational data are not yet sufficient to investigate whether in stars with both anomalies different mixing parameters would be needed, or whether one set could explain both (which is partially possible, see Denissenkov & Weiss 1996).

We add here that it was shown in parametric models (Weiss et al. 1996), that as a consequence of deep mixing the  $^3\text{He}$  produced in large amounts during the main-sequence and present in the convective envelope after the 1<sup>st</sup> du, will be transported to high enough temperatures to reduce it significantly to the much lower equilibrium abundances maintained there. This, in contrast to canonical theory, prevents low-mass stars from being effective  $^3\text{He}$ -producers and reconciles theoretical predictions with observations of  $^3\text{He}$ -abundances as function of galactic radius, i.e. chemical evolution (see also Charbonnel 1995).

#### 4.2. Meridional circulation

In the initial paper by Sweigart & Mengel (1979) meridional circulation was invoked to explain observed  $^{12}\text{C}/^{13}\text{C}$ -anomalies. Charbonnel (1995) used the same physical picture, but calculated the stellar evolution and mixing self-consistently for given angular momentum distribution. The mixing depth depends crucially on the molecular weight gradient, i.e. composition changes. While theoretical estimates are available, one can also determine the critical value from comparison with observations. We show in Fig. 8 the result obtained by Charbonnel et al. (1998), in which it was demonstrated that estimated

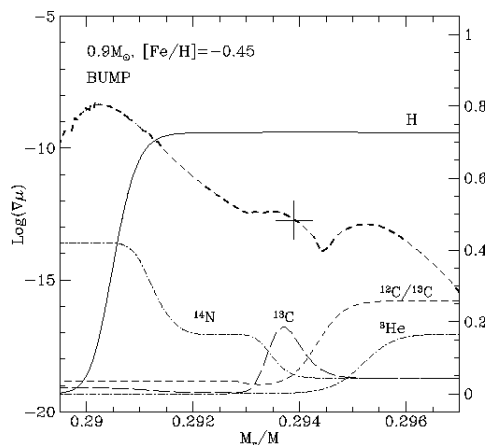


**Fig. 8.** Hydrogen-shell composition and molecular weight gradient (dashed line) in a low-mass stellar model after the bump, and critical position (cross) down to which deep mixing is allowed to reproduce observed  $^{12}\text{C}/^{13}\text{C}$ -values (from Charbonnel et al. 1998). Before the bump, the same critical value is reached in regions outside of CN-processed layers.

critical gradients agree with depths necessary to explain  $^{12}\text{C}/^{13}\text{C}$ -observations, and that only after the bump mixing to this point leads to surface abundance variations. This strengthens the case for rotation being a, if not the reason for deep mixing.

#### 4.3. Rotation-induced mixing

The most widely used description of rotation useful for full stellar evolution calculations is the one based on Zahn (1992), in the version of Maeder & Zahn (1998). Though there are several modifications to the basic theory, we will not enter into the details here. The fundamental point is that the interaction of meridional circulation with turbulence caused by the differential rotation and the feedback of angular momentum transport is taken into account. Therefore, this theory opens the possibility to consistently include rotation and all resulting effects, notably the transport of species, in stellar evolution calculations. It has been used successfully for massive stars (Meynet & Maeder

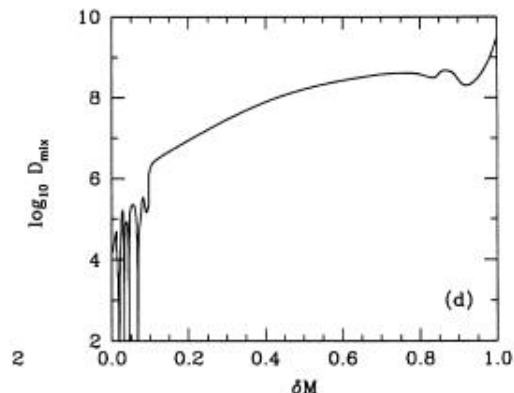


**Fig. 9.** Effective  $D_{\text{mix}}$ , obtained in the calculations by Denissenkov & Tout (2000) from the rotation theory of Maeder & Zahn, in the region above the hydrogen shell of a low-mass red giant.

2003 and references therein), and recently also for explaining the blue side of the Li-dip in open clusters (Palacios et al. 2003).

The same theory has been used by Denissenkov & Tout (2000), but with the post-processing approach, i.e. without full inclusion in the stellar models. We show in Fig. 9 the resulting effective  $D_{\text{mix}}$ , which is in nice agreement with the values used in the parametric approaches. The mixing depth also is in agreement with previous estimates to successfully explain the O-Na-anticorrelation (see Fig. 7, solid line).

These good news, however, are not confirmed by the models of Palacios et al. (2003a, in preparation), who use the same program as Palacios et al. (2003) and Palacios (2002). In these calculations the back-reaction of rotationally induced mixing is fully taken into account. The initial surface rotation velocity on the main-sequence was set to 5 km/s, which reduces to values below 0.5 km/s on the RGB. No deep mixing on the RGB is obtained, because effective diffusive speeds are much too low. One point of uncertainty is that the convective envelope is assumed to be in solid-body rotation. Assuming constant specific angular momentum instead (see Sills & Pinsonneault 2000), the interaction of the inner boundary

of the convective region with rotation leads to  $D_{\text{mix}}$  higher by a few orders of magnitude. Nevertheless, the extra mixing does not take place. The authors argue that already on lower part of the RGB, some modification of composition profiles take place and that this may be the reason for mixing speeds still lower than those found by Denissenkov & Tout (2000), and too low for substantial deep mixing on the RGB.

### 5. The Li-flash

While in Sect. 2 we have mentioned Li-depletion on the RGB as a signature for deep mixing, we now turn to the opposite anomaly – the super Li-rich giants, which are low-mass stars (of various metallicities) displaying  ${}^7\text{Li}$ -abundances well above the primordial level and any canonical prediction. According to Charbonnel & Balachandran (2000) they cluster predominantly at the bump, although very luminous objects have been observed, too (see Denissenkov & Weiss 2000 and references therein). The results by Palacios et al. (2003a, in preparation) and Palacios et al. (2001) indicate that rotation, deep mixing, and a transient episode of Li-enrichment are all connected:

The sequence of events, as indicated by the calculations, starts with slow ( $D_{\text{mix}} \gtrsim 10^8$ , as given by rotation theory) deep-mixing of  ${}^3\text{He}$  into the outer shell regions, where it is quickly burnt to  ${}^7\text{Be}$  as part of the  $pp$ -II-chain. The freshly produced  ${}^7\text{Be}$  is transported outwards, but decays already at such temperatures that the product  ${}^7\text{Li}$  is burnt by proton-capture to  $2\ {}^4\text{He}$  nuclei. The Li-energy release is large, such that a “Li-shell” is established, whose energy production rate rivals that of the  $pp$ -chain for a short time. The energy release, according to the rotation theory, interacts with the rotation, such that the vertical mixing speed is greatly enhanced, and new  ${}^7\text{Li}$  is now transported into the convective envelope: a super Li-rich giant is the result. The same mixing erases any molecular gradients, such that even after the Li-flash, mixing with the comparably low  $D_{\text{mix}}$  is able to lead to the observed CN-variations at the surface. While this is a very nice scenario, it seems to depend sensitively on

details in the computations and the initial composition, because Denissenkov (private communication) could not reproduce this sequence of events. This therefore needs further investigation.

### 6. Conclusions

It is now beyond doubt, that there exists a mechanism for transporting matter between the hydrogen-burning shell and the convective envelope in basically all low-mass red giants, which is not part of the standard canonical evolution theory. The result of this extra- or deep mixing are modifications in the abundances of isotopes participating in the  $pp$ -chains ( ${}^7\text{Li}$ ,  ${}^3\text{He}$ ), and CNO-cycle (C, N,  ${}^{12}\text{C}/{}^{13}\text{C}$ ). It is also evident that the deep mixing starts at the red giant bump, that is at the time when molecular weight barriers are minimal. Abundance anomalies of isotopes of higher  $p$ -burning cycles (O, Na, Mg, Al) appear to be mostly of primordial origin according to the present observational evidence, the source and the details of how they get into the observed stars still awaiting clarification.

Stellar evolution theory thus needs to be extended by a physical mechanism that pro-

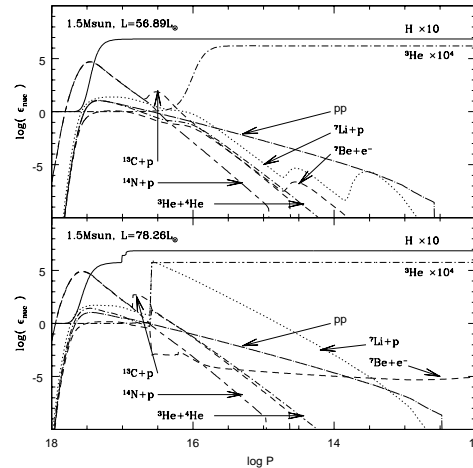


**Fig. 10.** Contributions to the energy generation before and during the Li-flash (Palacios et al. 2001).



vides the extra-mixing. Most promising is rotation, where big advances have been made during the last 10 years. Models which are almost or completely self-consistent are appearing and first results are promising. The Li-flash is an interesting possibility to explain the onset of deep mixing. The rotation theory itself, though certainly inferior to a full 3d-hydro-simulation appears to be a description accurate enough to allow trustworthy stellar evolution calculations.

*Acknowledgements.* A.W. was supported in part by a travel grant from the *Deutsche Forschungsgemeinschaft*.

## References

- Balachandran, S. & Carr, J. 2003, in ASP conf. series, Vol. 304, CNO in the Universe, ed. C. Charbonnel, D. Schaerer, & G. Meynet (San Francisco: Astron. Soc. Pacific), 101
- Bellman, S., Briley, M. M., Smith, G. H., & Claver, C. F. 2001, *PASP*, 113, 326
- Boothroyd, A. I. & Sackmann, I.-J. 1999, *ApJ*, 510, 232
- Cavallo, R. M., Sweigart, A. V., & Bell, R. A. 1996, *ApJ*, 464, L79
- Charbonnel, C. 1995, *ApJL*, 453, L41
- Charbonnel, C. & Balachandran, S. C. 2000, *A&A*, 359, 563
- Charbonnel, C., Brown, J. A., & Wallerstein, G. 1998, *A&A*, 332, 204
- Charbonnel, C. & do Nascimento, J. D. 1998, *A&A*, 336, 915
- Clayton, D. D. 1983, *Principles of stellar evolution and nucleosynthesis*, 2nd edn. (Chicago: Univ. of Chicago Press)
- Denissenkov, P. A., Da Costa, G. S., Norris, J. E., & Weiss, A. 1998, *A&A*, 333, 926
- Denissenkov, P. A. & Denissenkova, S. N. 1990, *SvA Lett.*, 16, 275
- Denissenkov, P. A. & Tout, C. A. 2000, *MNRAS*, 316, 395
- Denissenkov, P. A. & Weiss, A. 1996, *A&A*, 308, 773
- Denissenkov, P. A. & Weiss, A. 2000, *A&A Letters*, 348, L49
- Gilroy, K. K. 1989, *ApJ*, 347, 835
- Gilroy, K. K. & Brown, J. A. 1991, *ApJ*, 371, 578
- Gratton, R. G., Bonifacio, P., Bragaglia, A., et al. 2001, *A&A*, 369, 87
- Gratton, R. G., Sneden, C., Carretta, E., & Bragaglia, A. 2000, *A&A*, 354, 169
- Grundahl, F., Briley, M., Nissen, P. E., & Feltzing, S. 2002, *A&A*, 385, L14
- Iben, I. 1965, *ApJ*, 142, 1447
- Ivans, I. I., Sneden, C., Kraft, R. P., et al. 1999, *AJ*, 118, 1273
- Kraft, R. P. 1994, *PASP*, 106, 553
- Kraft, R. P., Sneden, C., Langer, G. E., & Shetrone, M. D. 1993, *AJ*, 106, 1490
- Langer, G. E. & Hoffman, R. D. 1995, *PASP*, 107, 1177
- Maeder, A. & Zahn, J.-P. 1998, *A&A*, 334, 1000
- Meynet, G. & Maeder, A. 2003, *A&A*, 404, 975
- Palacios, A. 2002, PhD thesis, Université Paul Sabatier, Toulouse
- Palacios, A., Charbonnel, C., & Forestini, M. 2001, *A&A*, 375, L9
- Palacios, A., Talon, S., Charbonnel, C., & Forestini, M. 2003, *A&A*, 399, 603
- Ramírez, S. V. & Cohen, J. G. 2002, *AJ*, 123, 3277
- Shetrone, M. D. 2003, *ApJL*, 585, L45
- Sills, A. & Pinsonneault, M. H. 2000, *ApJ*, 540, 489
- Sweigart, A. V. & Mengel, K. G. 1979, *ApJ*, 229, 624
- Wasserburg, G. J., Boothroyd, A. I., & Sackmann, I. J. 1995, *ApJ Letters*, 447, 37
- Weiss, A., Denissenkov, P. A., & Charbonnel, C. 2000, *A&A*, 356, 181
- Weiss, A., Wagenhuber, J., & Denissenkov, P. A. 1996, *A&A*, 313, 581
- Zahn, J.-P. 1992, *A&A*, 265, 115
- Zoccali, M., Cassisi, S., Piotto, G., & Salaris, G. B. M. 1999, *ApJL*, 518, L49